Acta Crystallographica Section D
Biological Crystallography
ISSN 0907-4449

Structure of C-phycocyanin from *Spirulina platensis* at 2.2 Å resolution: a novel monoclinic crystal form for phycobiliproteins in phycobilisomes

Xin-Quan Wang,[a] Le-Nong Li,[b] Wen-Rui Chang,[a] Ji-Ping Zhang,[a] Lu-Lu Gui,[a] Bao-Jiang Guo[b] and Dong-Cai Liang[a]*

[a]National Laboratory of Biomacromolecules, Institute of Biophysics, Chinese Academy of Sciences, 15 Datun Road, Chaoyang District, Beijing 100101, People's Republic of China, and [b]Institute of Biotechnology, Huanan Normal University, Guangzhou 510631, People's Republic of China

Correspondence e-mail: dcliang@sun5.ibp.ac.cn

Received 10 November 2000
Accepted 13 March 2001

PDB Reference: C-phycocyanin, 1gh0.

The crystal structure of C-phycocyanin from the cyanobacterium *S. platensis* has been determined at 2.2 Å resolution. The crystals belong to the monoclinic crystal form, which has not been previously reported for phycobiliprotein structures. The structure was solved using the molecular-replacement method with a final R value of 18.9% ($R_{\rm free}$ = 23.7%) after model building and refinement. In the crystals used for the study, the C-phycocyanin hexamers formed by face-to-face association of two trimers are arranged in layers rather than in columns. Three different kinds of packing between adjacent hexamers in the layer were compared. The tight packing of two adjacent hexamers formed by four trimers in the asymmetric unit brings β155 PCB chromophores close together, so it is possible that lateral energy transfer takes place through the β155–β155 route.

1. Introduction

The major light-harvesting capacity of prokaryotic cyanobacteria and eukaryotic red algae is associated with large antennae complexes, phycobilisomes, that are located on the surface of the photosynthetic membranes (Glazer, 1985; Bryant, 1991; MacColl & Guard-Friar, 1987; MacColl, 1998). Phycobilisomes are composed of rods and a core which are highly organized by various phycobiliproteins and linker polypeptides. Different phycobiliproteins contain different kinds and different numbers of chromophores, which are open-chain tetrapyrroles linked to cysteine residues *via* thioester bonds. The chromophores are classified by structure as phycoerythrobilin (PEB), phycocyanobilin (PCB), phycoviolobilin (PVB) and phycourobilin (PUB) (Bryant, 1991; Glazer, 1985). The phycobiliproteins can be divided into three major classes according to their spectral features: phycoerythrins (PE; $\lambda_{\rm max}$ = 565 nm), phycocyanins (PC; $\lambda_{\rm max}$ = 617 nm) and allophycocyanins (AP; $\lambda_{\rm max}$ = 650 nm).

All phycobiliproteins have a common subunit organization, which consists of α-and β-subunits that form a heterodimer $\alpha\beta$ (Apt *et al.*, 1995). The heterodimer, called a 'monomer' in the phycobiliprotein assembly pathway, can aggregate together to form disc-shaped $(\alpha\beta)_3$ trimers. The $(\alpha\beta)_6$ hexamer is formed by tight association of two $(\alpha\beta)_3$ trimers (Glazer, 1989; Glazer & Melis, 1987). The rods in phycobilisome normally include two or more phycocyanin hexamers, but in some species rods also contain phycoerythrin or phycoerythrocyanin hexamers located at the rod tips. The phycobilisome core, which contacts with the thylakoid membrane, is composed of two or three rods built from spectroscopically distinct allophycocyanins and linker polypeptides.

Phycocyanin has three PCB chromophores attached to the $\alpha\beta$ monomer through thioester linkages at the α84, β84 and

β155 positions. As a major component of the rods, the hexameric phycocyanins not only absorb light energy, but also transfer the energy from phycoerythrins to allophycocyanins in the core. The energy is then transferred to the photosynthesis reaction centre. The energy transfer from the phycobilisomes to the photosynthesis reaction centres within the thylakoid membrane is a very fast and effective process (Gantt, 1990).

The first solved structure of phycobiliprotein was that of C-phycocyanin from *Mastigocladus laminosus* (Schirmer *et al.*, 1985). Other reported phycocyanin structures include C-phycocyanin from *Agmenellum quadruplicatum* (Schirmer *et al.*, 1986), C-phycocyanin from *Fremyella diplosiphon* (Duerring *et al.*, 1991) and C-phycocyanin from *Cyanidium caldarium* (Stec *et al.*, 1999). The solved phycoerythrin structures include B-phycoerythrin from *Porphyridium sordidum* (Ficner *et al.*, 1992), R-phycoerythrin from *Polysiphonia urceolata* (Chang *et al.*, 1996) and R-phycoerythrin from *Griffithsia monilis* (Ritter *et al.*, 1999). Reported allophycocyanin structures include allophycocyanins from *S. platensis*, *Porphyra yezoensis* and *M. laminosus* (Brejc *et al.*, 1995; Liu *et al.*, 1999; Reuter *et al.*, 1999). All the structures are very similar.

The crystal structure of C-phycocyanin from *S. platensis* described here has been determined at 2.2 Å resolution. The crystals belong to the monoclinic system, which is a new crystal form for phycocyanin and also a novel form for reported phycobiliprotein structures. There are four C-phycocyanin $(\alpha\beta)_3$ trimers, which aggregate face-to-face to form two $(\alpha\beta)_6$ hexamers in the asymmetric unit. The packing between these two adjacent hexamers is different from that found in other phycocyanins. The relatively tight packing and the short distance between β155 PCB chromophores of adjacent hexamers suggest that β155 plays an important role in the lateral energy transfer in phycobilisomes.

2. Materials and methods

2.1. Crystallization of C-phycocyanin from *S. platensis*

S. platensis C-phycocyanin crystals were grown using the hanging-drop vapour-diffusion method at room temperature in the dark. The hanging drops contained 6.5 mg ml^{-1} C-phycocyanin in 100 m*M* phosphate buffer pH 6.8, 8%(*v*/*v*) saturated $(NH_4)_2SO_4$, 3%(*v*/*v*) saturated NaCl and 1.25%(*v*/*v*) MPD. The well solution contained 25%(*v*/*v*) saturated $(NH_4)_2SO_4$ and 100 m*M* phosphate buffer pH 6.8. The crystal dimensions reached 0.65 × 0.40 × 0.15 mm after 4–5 weeks.

2.2. Data collection and processing

X-ray diffraction data were collected with a Weissenberg camera (Sakabe, 1991) installed on beamline 16B at the KEK Photon Factory. A total of 65 frames (size 400 × 800 mm) with an oscillation angle of 3.5° were collected with a wavelength of 1.0 Å. The crystal-to-detector distance was 573 mm. The intensities between 20.0 and 2.2 Å were integrated and equivalent reflections were merged using the programs *DENZO* and *SCALEPACK* (Otwinowski & Minor, 1997). Details of the crystal parameters and data-processing statistics are given in Table 1.

2.3. Molecular replacement

The amino-acid sequences of the α-chain (SWISS-PROT database accession No. P72509) and the β-chain (SWISS-PROT database accession No. P72508) of C-phycocyanin from *S. platensis* were aligned with those of C-phycocyanin from *F. diplosiphon* (Fig. 1). The identities were 80.9 and 79.7%, respectively. A C-phycocyanin $(\alpha\beta)_3$ trimer model was constructed by rotating the $(\alpha\beta)$ monomer of *F. diplosiphon* around the three-dimensional axis, with differing residues replaced by alanine. Rotation and translation functions were calculated using the *AMoRe* program and the constructed model (Navaza, 1994) (Table 2).

```
alpha_Fredi     MKTPLTEAVA AADSQGRFLS STEIQTAFGR FRQASASLAA AKALTEKASS
alpha_Spiru     MKTPLTEAVS IADSQGRFLS STEIQVAFGR FRQAKAGLEA AKALTSKADS
alpha_model     MKTPLTEAVS VADSQGRFLS STEIQVAFGR FRQAKAGLEA AKALTSKADS

                                                *
alpha_Fredi     LASGAANAVY SKFPYTTSQN GPNFASTQTG KDKCVRDIGY YLRMVTYCLV
alpha_Spiru     RISGAAQAVY NKFPYTTQMQ GPNYAADQRG KDKCARDIGY YLRMVTYCLI
alpha_model     LISGAAQAVY NKFPYTTQMQ GPNYAADQRG KDKCARDIGY YLRMVTYCLI

alpha_Fredi     VGGTGPLDDY LIGGIAEINR TFDLSPSWYV EALKYIKANH GLSGDPAVEA
alpha_Spiru     AGGTGPMDEY LIAGIDEINR TFELSPSWYI EALKYIKANH GLSGDAAGEA
alpha_model     AGGTGPMDEY LIAGIDEINR TFELSPSWYI EALKYIKANH GLSGDAAVEA

alpha_Fredi     NSYIDYAINA LS
alpha_Spiru     NSYLDYAINA LS
alpha_model     NSYLDYAINA LS

beta_Fredi      MLDAFAKVVS QADARGEYLS GSQIDALSAL VADGNKRMDV VNRITGNSST
beta_Spiru      MFDAFTKVVS QADTRGEMLS TAQIDALSQM VAESNKRLDA VNRITSNAST
beta_model      MFDAFTKVVS QADTRGEMLS TAQIDALSQM VAESNKRLDV VNRITSNAST

                                                *
beta_Fredi      IVANAARSLF AEQPQLIAPG GNAYTSRRMA ACLRDMEIIL RYVTYAIFAG
beta_Spiru      IVSNAARSLF AEQPQLIAPG GNAYTNRRMA ACLRDMEIIL RYVTYAVFAG
beta_model      IVSNAARSLF AEQPQLIAPG GNAYTSRRMA ACLRDMEIIL RYVTYAVFAG

beta_Fredi      DASVLDDRCL NGLKETYLAL GTPGSSVAVG VQKMKDAALA IAGDTNGITR
beta_Spiru      DASVLEDRCL NGLRETYLAL GTPGSSVAVG VGKMKEAALA IVNDPAGITP
beta_model      DASVLEDRCL NGLRETYLAL GTPGSSVAVG VGKMKEAALA IVNDPAGITP

                *
beta_Fredi      GDCASLMAEV ASYFDKAASA VA
beta_Spiru      GDCSALASEI ASYFDRACAA VS
beta_model      GDCSALASEI AGYFDRAAAA VS
```

Figure 1
Alignment of the C-phycocyanin amino-acid sequences for *F. diplosiphon*, *S. platensis* (from SWISS-PROT database) and our model. The non-identical residues between the sequence from *F. diplosiphon* and that from the database are shown in bold. The differing residues between the model sequence and that from the database are underlined. The cysteinyl attachments for the chromophores are marked with an asterisk.

Table 1
Crystal parameters and data-collection statistics.

Values for the highest resolution shell (2.25–2.20 Å) are listed in parentheses.

Space group	$P2_1$
Unit-cell parameters	
a (Å)	109.0
b (Å)	117.5
c (Å)	185.0
β (°)	90.3
No. of trimers per asymmetric unit	4
Resolution range (Å)	20.0–2.2
No. of unique reflections	224259 (14756)
$I/\sigma(I)$	13.1 (2.7)
Redundancy	2.1
Completeness (%)	95.4 (94.4)
$R_{\rm merge}$	7.5 (31.3)
Reflections with $I/\sigma(I) > 2$ (%)	76.0 (51.3)

2.4. Refinement

Refinement was carried out using the *X-PLOR* program (Brünger, 1992) in the resolution range 20.0–2.2 Å with the geometrical parameters restrained to those proposed by Engh & Huber (1991). 5% of the reflections were selected randomly to check the course of refinement by calculating the $R_{\rm free}$ value (Brünger, 1997). Bulk-solvent corrections of the diffraction data were applied according to the procedure described by Jiang & Brünger (1994) (k = 0.33 e Å^{-3}, B = 67 Å^2).

The $R_{\rm free}$ and R values of the initial model after the molecular-replacement method were 39.4 and 38.9%, respectively. After one cycle of rigid-body and positional refinement, the $R_{\rm free}$ and R values fell to 32.6 and 28.1%. According to the $2|F_o| - |F_c|$ and $|F_o| - |F_c|$ electron-density maps, the chromophores were added and residues differing between C-phycocyanin of *S. platensis* and that of *F. diplosiphon* were adjusted using the program *O* (Jones *et al.*, 1991). Several cycles of positional refinement, simulated-annealing with the slow-cool protocol and individual isotropic temperature-factor refinement were conducted, with each cycle followed by manual rebuilding based on the $2|F_o| - |F_c|$ and $|F_o| - |F_c|$ maps. The $R_{\rm free}$ and R values fell to 27.2 and 21.2%, respectively. Water molecules were added to the model at locations with $|F_o| - |F_c|$ electron densities greater than 3σ and hydrogen-bonding stereochemistry. A total of 945 water molecules were added to the model. The final $R_{\rm free}$ and R values were 23.7 and 18.9%, respectively, in the resolution range 20.0–2.2 Å. The refinement statistics are listed in Table 3.

3. Results and discussions

3.1. Data processing and molecular replacement

The unit-cell parameters are a = 109.0, b = 117.5, c = 185.0 Å, β = 90.3°. The β angle is very close to 90°. In the early data-processing stages, the crystal system was determined to be orthorhombic. In reciprocal space, the $R_{\rm merge}$ values of the equivalent reflections around the mirror planes (hk0), (0kl) and (h0l) were 41, 41 and 6%, respectively. The high $R_{\rm merge}$ values for the mirror planes (hk0) and (0kl) indicate that the

Table 2
Molecular replacement.

All calculations were carried out with data in the 8.0–4.0 Å resolution range. Values in parentheses are the highest noise peaks.

	α	β	γ	x	y	z	CC	R
Rotation function								
1	272.83	95.07	39.17				15.8	
4	267.17	84.93	219.17				15.8	
7	93.40	86.05	103.55				15.2	
10	86.60	93.95	283.55				15.2	
Two-body translation function								
Fix 1	272.83	95.07	39.17	0.3000	0.0000	0.4107		
4a	267.17	84.93	219.17	0.6833	0.0241	0.9197	21.3 (13.4)	51.3 (60.5)
4b	267.17	84.93	219.17	0.7038	0.4999	0.5910	16.4 (13.4)	51.6 (60.5)
7a	93.40	86.05	103.55	0.2826	0.2084	0.4216	25.2 (12.7)	48.8 (52.0)
7b	93.40	86.05	103.55	0.3027	0.7383	0.0860	24.0 (12.7)	49.0 (52.0)
10a	86.60	93.95	283.55	0.7174	0.7084	0.5784	25.2 (14.0)	48.8 (52.0)
10b	86.60	93.95	283.55	0.6973	0.2383	0.9140	24.0 (14.0)	49.0 (52.0)
Rigid-body refinement								
1	273.23	97.26	39.15	0.2954	0.0036	0.4080	62.7	35.6
7a	93.07	83.30	103.54	0.2827	0.2083	0.4236	62.7	35.6
4a	266.92	87.99	219.22	0.6852	0.0311	0.9183	62.7	35.6
10b	86.97	90.89	283.50	0.6961	0.2388	0.9152	62.7	35.6

Laue symmetry is 2/m. Combined with the symmetric absences along the 0k0 axis, the space group was determined to be $P2_1$. The crystals were estimated to contain 24 $\alpha\beta$ monomers in the unit cell, with a $V_{\rm M}$ of 2.42 Å^3 Da^{-1} and a solvent content of 43% (Matthews, 1968). The 12 $\alpha\beta$ monomers in the asymmetric unit can form four $(\alpha\beta)_3$ trimers.

The molecular-replacement method was conducted using diffraction data in the resolution range 8–4 Å. The rotation-function calculations resulted in 12 peaks with relatively high CC values. Because of the local threefold axis in the trimer, only peaks 1, 4, 7 and 10 are independent solutions which represent the orientations of the four trimers in the asymmetric unit. The one-body translation-function calculations gave individual solutions for peaks 1, 4, 7 and 10. After fixing solution 1, two-body translation-function calculations gave two distinct solutions for peaks 4, 7 and 10. Analysis of these solutions indicated that solutions 7a and 10a, 7b and 10b, 4b and fixed solution 1 were all related by the crystallographic 2_1 axis. The final four solutions were 1, 4a, 7a and 10b. After rigid-body refinement, the CC value was 0.63 and the R value was 36%. Observation of the packing on an SGI graphical workstation indicated that the four trimers determined by the final four solutions were arranged in 222 symmetry. The non-crystallographic twofold axis relating solutions 1 and 4a, 7a and 10b is parallel to the crystallographic 2_1 axis, with its position in the cell being (0.49, y, 0.65). Because of the existence of the non-crystallographic twofold axis, the two-body translation function gave two distinct solutions for peaks 4, 7 and 10, with these solutions related by the crystallographic 2_1 axis as mentioned above. The self-rotation function was calculated using program *POLARRFN* from the *CCP*4 suite (Collaborative Computational Project, Number 4, 1994) with radius 30 Å and diffraction data in the resolution range 8–5 Å. The peak of the non-crystallographic twofold axis mentioned above is masked by the self-peak. The peaks of the other two

Table 3
Refinement statistics.

Values for the highest resolution shell (2.30–2.20 Å) are given in parentheses.

Resolution range (Å)	20.0–2.2
No. of reflections	224259 (14756)
$F/\sigma(F)$ cutoff	0.0
R factor	18.9 (25.7)
R_{free} factor (5% of data)	23.7 (29.1)
Number of non-H atoms	
Protein	30000
Chromophore	1548
Water	945
Root-mean-square deviations	
Bond lengths (Å)	0.007
Bond angles (°)	1.1
Dihedral angles (°)	20.7
Improper angles (°)	0.7
Temperature factors (Å^2)	
Protein	22.5
Main-chain atoms	21.3
Side-chain atoms	23.8
Chromophore	22.2
Water	33.0

non-crystallographic twofold axis are at polar angles (ψ = 30, ω = 0, κ = 180°) and (ψ = 120, ω = 0, κ = 180°).

3.2. Model quality

The final four $(\alpha\beta)_3$ trimers model contains 30 000 non-H protein atoms, 1548 chromophore atoms and 945 water molecules. The final R value is 18.9% for the 224 259 unique reflections in the resolution range 20.0–2.2 Å; R_{free} for 5% of the total reflections is 23.7%. R.m.s. deviations from the ideal values of the bond lengths and bond angles are 0.007 Å and 1.1°, respectively. The average B-factor statistics are listed in Table 3. In the Ramachandran plot (Fig. 2) (Ramachandran *et al.*, 1963), 95.3% of the non-Gly and non-Pro residues fall into the most favoured regions, with the exception being Thr75 in the β-chain. Thrβ75 falls into the disallowed region because of its close contact with chromophore α84 in the neighbouring monomer. Its dihedral angles are highly conserved among all phycobiliprotein structures (Schirmer *et al.*, 1985, 1986; Duerring *et al.*, 1991; Brejc *et al.*, 1995; Chang *et al.*, 1996; Stec *et al.*, 1999).

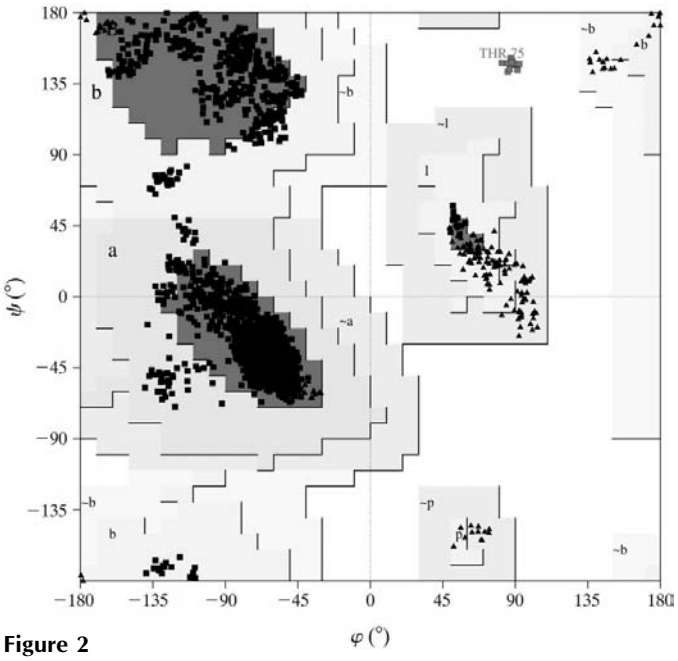

Figure 2
Ramachandran plot of the *S. platensis* C-phycocycnin residues calculated by *PROCHECK* (Laskowski *et al.*, 1993). Glycine residues are marked as triangles. Non-glycine residues are marked as squares. Of 3540 non-glycine and non-proline residues, 3375 (95.3%) are in the most favoured regions (A, B, L) and 153 (4.3%) are in the additional allowed regions (a, b, l, p). β-Subunit Thr75 residues (12; 0.3%) are in the disallowed regions.

3.3. Description of the structure

The asymmetric unit of C-phycocyanin from *S. platensis* contains four $(\alpha\beta)_3$ trimers. The four $(\alpha\beta)_3$ trimers aggregate face-to-face to form two $(\alpha\beta)_6$ hexamers, referred to in the text as hexA and hexB. The centre of mass of hexA is (31.08, 12.34, 76.89) and that of hexB is (74.47, 15.94, 169.52). HexA and hexB in the asymmetric unit are arranged side by side, but they are not at the same level parallel to the plane (x0z) (Fig. 3). Because the angle between the least-squares planes of these two hexamers is about 4° (Fig. 3), the local twofold axis is not an exact twofold axis, but the deviation is small. This arrangement again shows that the space group is $P2_1$ and not $P22_12$. The modular structure of the C-phycocyanin hexamer from *S. platensis* is an $\alpha\beta$ monomer. The α-chain contains 162

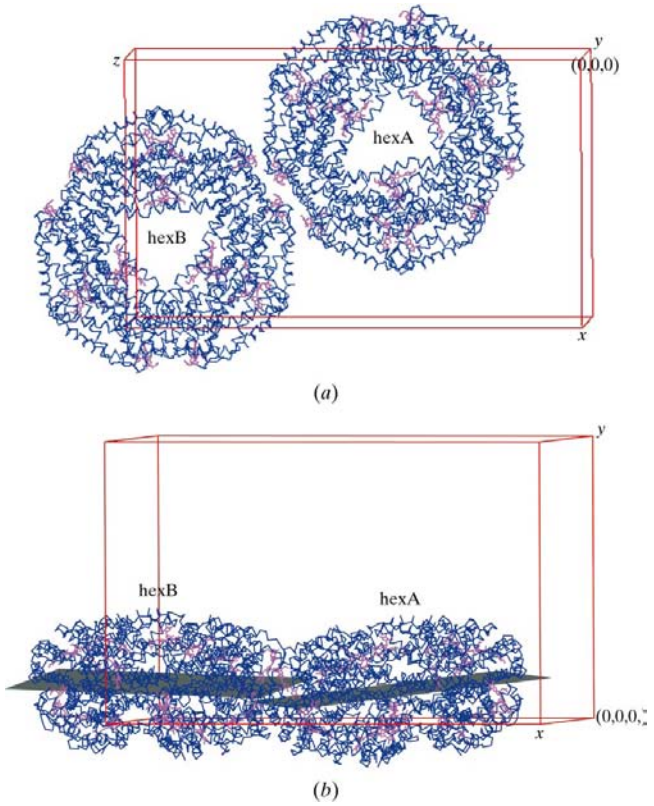

Figure 3
Two *S. platensis* C-phycocyanin hexamers in the asymmetric unit. (*a*) View along the *b* axis; (*b*) view along the *a* axis. Note that the least-squares planes of hex1 and hex2, indicated by the planes, are not parallel.

residues and the β-chain contains 172 residues. The α- and β-subunits have similar three-dimensional structures, including nine helices (*X*, *Y*, *A*, *B*, *E*, *F*′, *F*, *G* and *H*) and loop linkages. In one $\alpha\beta$ monomer, three PCB chromophores (Fig. 4) are covalently attached to cysteine residues by thioester bonds.

HexA and hexB include 12 $\alpha\beta$ monomers, which contain 24 polypeptides named from *A* to *X*. The 12 monomers are *AB*, *CD*, *EF*, *GH*, *IJ*, *KL*, *MN*, *OP*, *QR*, *ST*, *UV* and *WX*. Pairwise C^{α} superposition of the 12 α-chains (*A*, *C*, *E*, *G*, *I*, *K*, *M*, *O*, *Q*, *S*, *U*, *W*) results in an average r.m.s. difference of 0.26 Å. For the 12 β-chains (*B*, *D*, *F*, *H*, *J*, *L*, *N*, *P*, *R*, *T*, *V*, *X*), the average r.m.s. difference between C^{α} atoms is 0.30 Å. The two C-phycocyanin structures in the Protein Data Bank (PDB) are those from *F. diplosiphon* (PDB code 1cpc) and from *Cyanidium caldarium* (PDB code 1phn). The r.m.s. difference between the C^{α} atoms of chain *A* from monomer *AB* and those of the α-chain from 1cpc is 0.35 Å and the r.m.s. difference between the C^{α} atoms of chain *A* and those of the α-chain from 1phn is 0.58 Å. The r.m.s. differences between the C^{α} atoms of chain *B* from monomer *AB* and those of the β-chains from 1cpc and 1phn are 0.33 and 0.73 Å, respectively.

The primary sequences of C-phycocyanin from *S. platensis* were obtained genetically and were deposited in the SWISS-PROT database (accession Nos. P72508 and P72509). Alignment with C-phycocyanin from *F. diplosiphon* (Fig. 1) showed that there are 31 differing residues in the α-chain (19.1%) and 35 differing residues in the β-chain (20.3%). In the early refinement stages, these differing residues were replaced with Ala. While refinement was taking place, these residues were progressively adjusted according to the electron-density map. The final model sequences are shown in Fig. 1. The differing residues from *S. platensis* C-phycocyanin sequences in the database were Val11, Leu51 and Val148 in the α-chain and Val40, Ser76, Gly162 and Ala168 in the β-chain (Fig. 5). The methylation of Asn72 in the β-chain has been proposed to be conserved in phycobiliproteins and to be involved in energy transfer (Swanson & Glazer, 1990). In C-phycocyanin from *S. platensis*, the side chain of Asn72 in the β-chain was also found to be methylated (Fig. 5).

3.4. Chromophores

There are a total of 36 PCB chromophores in the asymmetric unit, which can be divided into three categories. To be consistent with PCB chromophore nomenclature, they are named α84, β84 and β155. Chromophore α84 is associated with Cys84 in the α-subunit, while the β84 and β155 PCB chromophores are linked to Cys82 and Cys153 in the β-subunit, respectively. The chromophores are attached to the protein by thioester bonds. All these chromophores in the *S. platensis* C-phycocyanin structure are well defined (Fig. 6) and the average temperature factors for α84, β84 and β155 are 16, 27 and 23 $Å^2$, respectively. Because the residues which interact with chromophore α84 (α-subunit: Asn73, Ala75, Lys83, Arg86 and Asp87; β-subunit of neighbouring monomer: Arg57, Thr75), β84 (β-subunit: Asn72, Arg77, Arg78 and Asp85) and β155 (β-subunit: Asn35, Asp39, Thr149 and Gly151) are conserved in *S. platensis* C-phycocyanin (Fig. 1), the structures of the individual α84, β84 and β155 superimpose well with their counterpart chromophores in 1cpc.

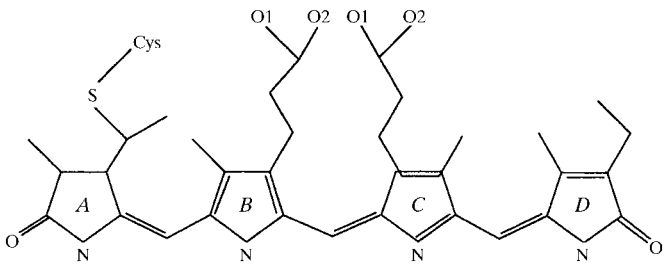

Figure 4
PCB chemical structure.

3.5. Crystal packing and protein contacts

Because of its tendency to form trimers and hexamers, most reported phycobiliprotein crystals belong to trigonal or hexagonal systems (Schirmer *et al.*, 1985, 1986; Duerring *et al.*, 1991; Ficner *et al.*, 1992; Chang *et al.*, 1996; Ritter *et al.*, 1999; Stec *et al.*, 1999; Brejc *et al.*, 1995; Liu *et al.*, 1999). Tetragonal

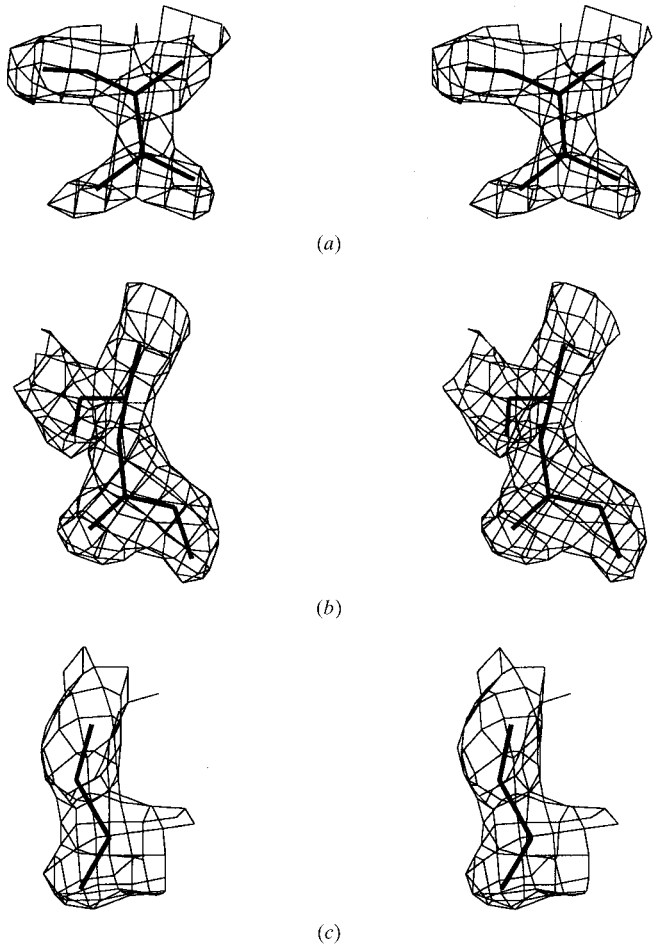

Figure 5
Stereo omit $2F_o - F_c$ electron-density maps of the residues in *S. platensis* C-phycocyanin. (*a*) Val*S*148; (*b*) γ-*N*-methylasparagine *B*72; (*c*) Gly*P*162.

Table 4
Amino-acid residues involved in the formation of *A*/*B*, *B*/*C* and *A*/*C* interfaces.

A/*B* interface (940 Å^2)		*B*/*C* interface (872 Å^2)		*A*/*C* interface (507 Å^2)	
HexA	*C* chain Ala138, Asn139, Gly141, Ser143; *D* chain Thr149; *I* chain Lys35; *J* chain Asp25, Ser28, Gln29, Ala32, Asn143, Pro145, Thr149, Pro150, Gly151, Asp152	HexB	*O* chain Tyr65, Gln68, Met69; *S* chain Gln57, Asn61, Lys62, Pro64, Thr67, Gln68, Lys81	HexA	*A* chain Gln57, Asn61, Pro64, Gln68, Gln70; *I* chain Asn61, Pro64, Gln68, Gln70
HexB	*O* chain Lys47, Ser143, Gly144; *P* chain Ala32, Lys36, Pro150, Gly151; *U* chain Arg32, Lys35, Glu39, Asp145; *V* chain Ala32, Thr149, Pro150, Gly151	HexC	*G* chain Ser53, Gln57, Ala58, Tyr60, Asn61, Thr67, Gln68, Ala76, Asn77, Gln78, Lys81	HexC	*E* chain Arg32, Lys35, Ser143, Asp145; *G* chain Lys35, Glu39; *H* chain Ala32, Glu33, Lys36, Thr149, Pro150, Gly151, Asp152

crystals of R-PC from *Polysiphonia urceolata* and orthorhombic crystals of allophycocyanin from *Chroomonas* species have also been reported (Zhang *et al.*, 1995; Reuter *et al.*, 1999). The C-phycocyanin structure from *S. platensis* described here is the first phycobiliprotein structure reported to belong to the monoclinic system. The upper and lower hexamers in the *S. platensis* C-phycocyanin crystals are offset (Fig. 7), whereas in *F. diplosiphon* C-phycocyanin crystals they are organized in columns. The crystallographic translational repeat along the hexamer column in the *F. diplosiphon* crystals is 61.24 Å. The hexamer–hexamer distance along the *b* axis in the *S. platensis* crystals is 58.75 Å (117.5 Å/2). The minimum distance between the C$^\alpha$ atoms of the upper and lower hexamer is 5.1 Å, while in the *F. diplosiphon* crystals it is 12.4 Å. These results show that the packing of the upper and lower hexamers in the *S. platensis* crystals is tighter than that in the *F. diplosiphon* crystals.

The hexamers are arranged in layers in the *S. platensis* C-phycocyanin crystals, which is like that in *Cyanidium caldarium* C-phycocyanin crystals (Fig. 8). Because of the different hexamer orientations in the layer, the hexamer side–side arrangements are not the same in the layer. The top hexamer is named hexA, with the other two hexamers named hexB and hexC in a clockwise direction. In the *C. caldarium* C-phycocyanin crystals, hexA, hexB and hexC are arranged along the crystallographic threefold *c* axis. The buried surface area between adjacent hexamers is about 500 Å^2 and is the same for the *A*/*B*, *B*/*C* and *A*/*C* interfaces. These three interfaces are made up of the same residues. HexA, hexB and hexC are absolutely equivalent in *C. caldarium* crystals. In *S. platensis* crystals, hexA and hexC are connected by a crystallographic translational repeat along the *a* axis. HexA and hexB in the asymmetric unit are related by the non-crystallographic twofold axis. The interactions along *A*/*B* involve chains *C*, *D*, *I* and *J* of hexA and chains *O*, *P*, *U* and *V* from hexB. The interaction residues are listed in Table 4. These residues form a buried surface area of 940 Å^2. The interactions along *B*/*C* are contributed by the α-subunit. The chains involved are chains *O* and *S* of hexB and chain *G* of hexC (Table 4). The buried surface area of the *B*/*C* interface is 872 Å^2. The surface area of the *A*/*C* interface is only 507 Å^2. The residues involved in the interactions are also shown in Table 4. Therefore, hexA (hexC) and hexB in *S. platensis* C-phycocyanin crystals are not absolutely equivalent but are quasi-equivalent.

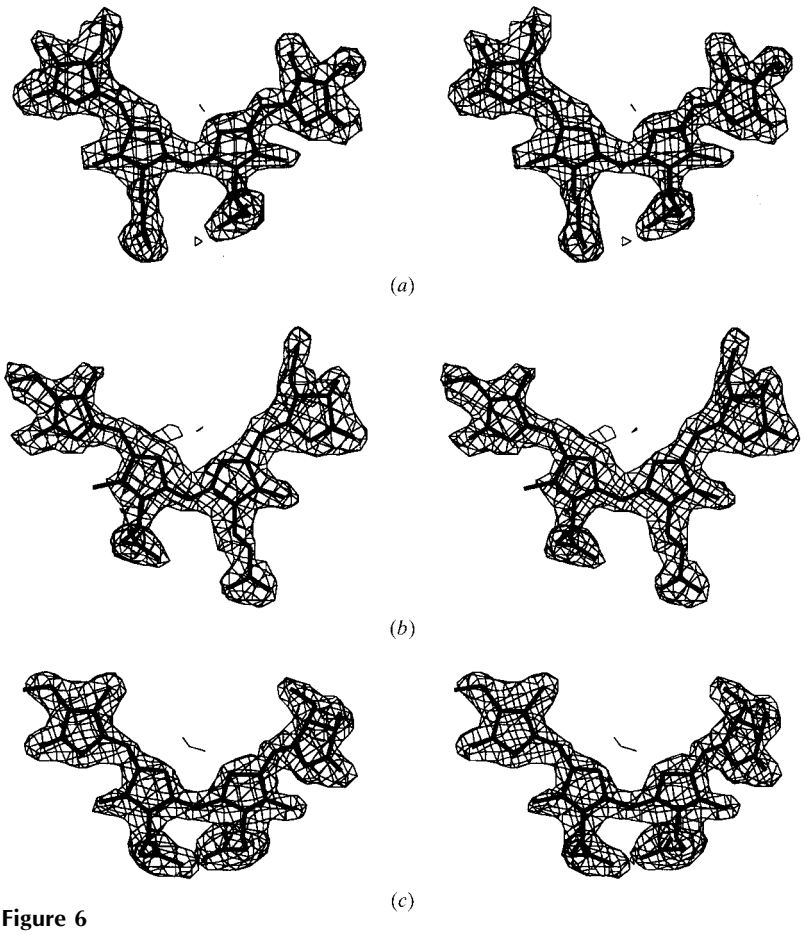

Figure 6
Stereo omit $2F_o - F_c$ electron-density maps of chromophores in *S. platensis* C-phycocyanin. (*a*) PCB α84; (*b*) PCB β84; (*c*) PCB β155.

3.6. Chromophore arrangements and energy pathways

The isolated chromophores tend to be cyclic and have low visible absorption. In phycobiliproteins, the attachment to the protein by

thioester bonds and the interactions with the surroundings cause the chromophores to be maintained in an extended state, which maximizes absorption in the visible region of the spectrum (Scheer & Kufer, 1977). In the C-phycocyanin ($\alpha\beta$) monomer, the three PCB chromophores have different spectral characteristics because of their different microenvironments (Debreczeny *et al.*, 1993). There is apparently one predominant mechanism, Förster resonance transfer in the weak coupling limit (Förster, 1967), that provides much of the chromophore–chromophore energy transfer.

We chose HexA as the example when measuring the distances between chromophores in one hexamer. The distances shorter than 50 Å between chromophores within the upper and lower trimers of HexA are listed in Table 5. The shortest distance is about 20 Å (α84–β84 on adjacent monomers). The distance between α84–β84 pairs around the trimer ring is about 34 Å. The distance β155–β84 on the same monomer is about 38 Å. Energy transfers within α84–β84 on adjacent monomers, within β155–β84 on the same monomer and within α84–β84 pairs around the trimer ring have been confirmed by the observed anisotropic fluorescence decay times for the three pathways of about 1.0, 50 and 40 ps, respectively (Debreczeny *et al.* 1995*a*,*b*). The other chromophore pairs with distances of about 40 Å are not main energy-transfer pathways because of disadvantageous orientation factors. Chromophores β155, β84 and α84 of adjacent monomers form a triangle (Fig. 9), which can be regarded as a light-harvesting functional unit in the trimer. In the functional unit, two higher energy chromophores, β155 and α84, which are located on the periphery of the trimer, transfer the energy to the lowest energy chromophore, β84 (Duerring *et al.*, 1991; Debreczeny *et al.*, 1995*a*,*b*).

When two trimers associate face-to-face to form a hexamer, new energy-migration pathways are opened (Schirmer *et al.*, 1986; Duerring *et al.*, 1991). The distances between the chromophores of the upper and lower trimers of *S. platensis* C-phycocyanin are listed in Table 6. The main energy-transfer pathways are α84(*A*)–α84(*I*), β84(*B*)–β84(*H*) and β155(*B*)–β155(*L*).

Three different kinds of interfaces *A*/*B*, *B*/*C* and *A*/*C* between adjacent hexamers in *S. platensis* C-phycocyanin crystals have been described above. In the hexamer *A*/*C* interface, the closest chromophore pair is α84(hexA)–β155(hexC), with a distance of about 26 Å. In the *B*/*C* interface, the closest chromophore pair is α84(hexB)–α84(hexC), with a distance of about 34 Å. The unique packing of hexA and hexB in the asymmetric unit brings the β155 chromophores very close together. The arrangement of the β155 chromophores in the *A*/*B* interface is shown in Fig. 10. The

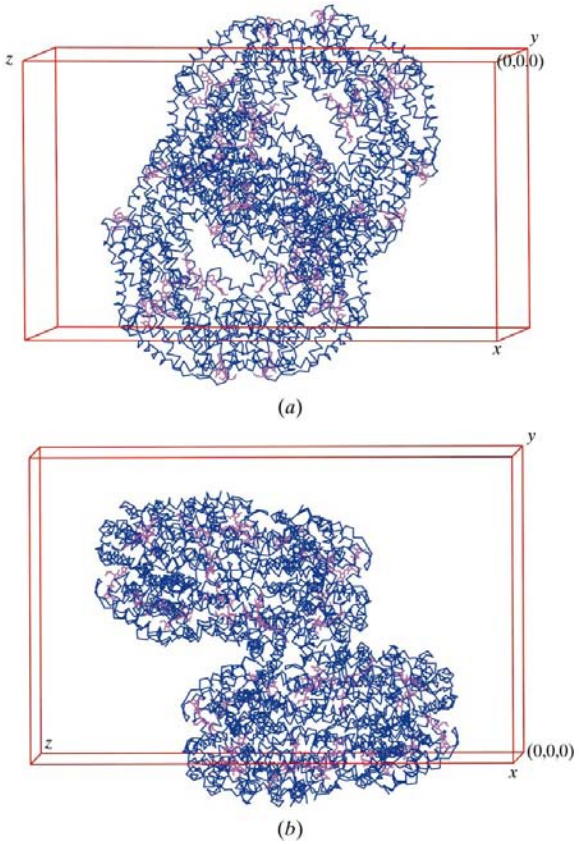

Figure 7
Packing of *S. platensis* C-phycocyanin hexamers along the *b*-axis direction. (*a*) View along the *b* axis; (*b*) view along the *a* axis.

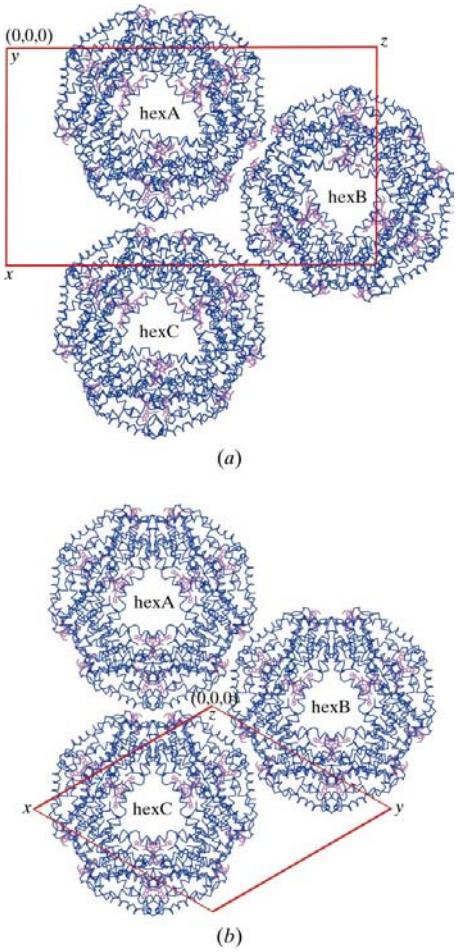

Figure 8
Packing of C-phycocyanin hexamers in the layer. (*a*) *S. platensis* C-phycocyanin; (*b*) *C. caldarium* C-phycocyanin (PDB code 1phn).

Table 5
Distances (<50 Å) between chromophores within the upper and the lower trimers in hexA.

Distances involved in energy transfer are given in bold.

Upper trimer.

	α84 (*A*)	β84 (*B*)	β155 (*B*)	α84 (*C*)	β84 (*D*)	β155 (*D*)	α84 (*E*)	β84 (*F*)	β155 (*F*)
α84 (*A*)			49.5		**20.4**	39.6			
β84 (*B*)			**38.7**		**34.3**		**20.1**	**34.2**	44.7
β155 (*B*)	49.5	**38.7**			46.9		39.6		
α84 (*C*)						49.9		**20.3**	36.8
β84 (*D*)	**20.4**	**34.3**	46.9			**38.3**		**34.7**	
β155 (*D*)	39.6			49.9	**38.3**			47.0	
α84 (*E*)		**20.1**	39.6						48.6
β84 (*F*)		**34.2**		**20.3**	**34.7**	47.0			**35.6**
β155 (*F*)		44.7		36.8			48.6	**35.6**	

Lower trimer.

	α84 (*G*)	β84 (*H*)	β155 (*H*)	α84 (*I*)	β84 (*J*)	β155 (*J*)	α84 (*K*)	β84 (*L*)	β155 (*L*)
α84 (*G*)			49.6		**20.3**	39.5			
β84 (*H*)			**38.8**		**34.7**		**20.2**	**34.3**	47.1
β155 (*H*)	49.6	**38.8**			46.9		39.8		
α84 (*I*)						50.0		**20.3**	39.1
β84 (*J*)	**20.3**	**34.7**	46.9			**38.5**		**34.4**	
β155 (*J*)	39.5			50.0	**38.5**			46.9	
α84 (*K*)		**20.2**	39.9						49.7
β84 (*L*)		**34.3**		**20.3**	**34.4**	46.9			**38.5**
β155 (*L*)		47.1		39.1			49.7	**38.5**	

closest distance, 13.6 Å, is between β155 (hexA) and β155 (hexB). This short distance makes very rapid energy transfer possible between the chromophores. The interaction surface

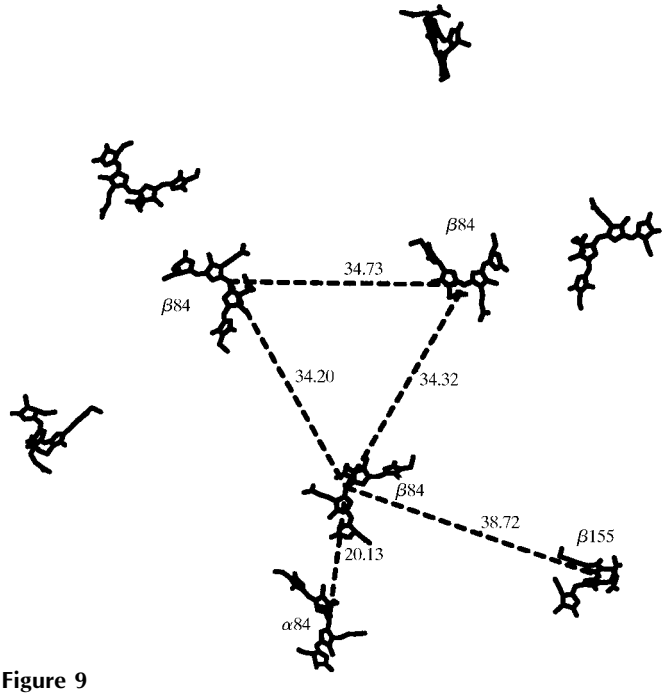

Figure 9
Chromophores arrangement in the *S. platensis* C-phycocyanin trimer. The energy-transfer function unit consists of PCB β155 and β84 belonging to the same monomer and α84 of the adjacent monomer. The length unit is Å.

Table 6
Distances (Å) between chromophores in the upper and lower trimers in hexA.

Distances involved in energy transfer are given in bold.

	α84 (*A*)	β84 (*B*)	β155 (*B*)
α84 (*G*)	76.4	59.6	89.9
β84 (*H*)	60.3	**34.0**	46.3
β155 (*H*)	89.8	45.7	74.1
α84 (*I*)	**26.9**	60.6	58.2
β84 (*J*)	61.6	48.3	72.7
β155 (*J*)	58.7	71.8	93.0
α84 (*K*)	70.9	36.0	40.6
β84 (*L*)	36.2	47.4	52.3
β155 (*L*)	40.1	52.3	**26.3**

area of *A*/*B* is about 940 Å, which is also the largest of these three different interfaces. These results suggest the possibility that hexA/hexB packing represents the lateral packing of the C-phycocyanin rods in the phycobilisome organelles and that lateral energy transfer is through the β155–β155 route.

The cysteine residue which connects the β155 chromophore is in the GH loop of the β-subunit. This chromophore connection site is located on the periphery of the phycobiliprotein hexamer and is only found in the phycobilisome rods (MacColl, 1998). The GH loop of allophycocyanin in the core is short and there is no cysteine residue which can connect to the chromophore, so there are only two chromophores, α84 and β84, in the allophycocyanin (αβ) monomer (Brejc *et al.*, 1995). In C-phycocyanin the β155 chromophore is PCB, whereas it is PEB in phycoerythrin. The short distance between β155 and α140a PEB chromophores of adjacent phycoerythrin hexamers offers a possible lateral energy-transfer pathway (Jiang *et al.*, 1999). The possible lateral

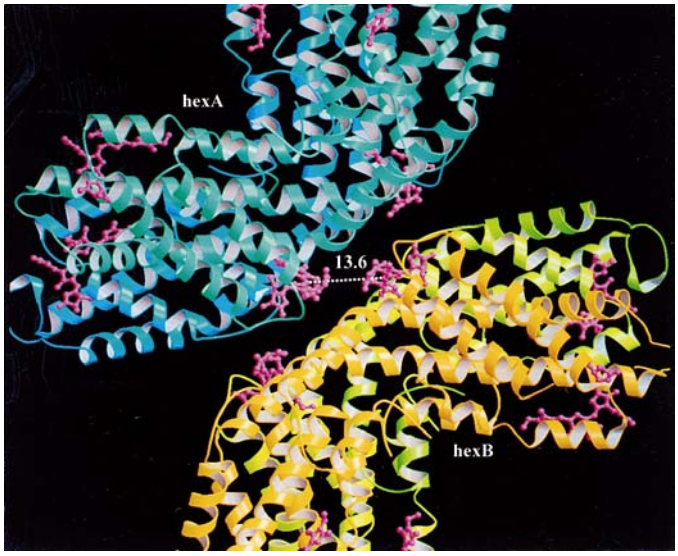

Figure 10
Arrangement of chromophores at the interface between *S. platensis* C-phycocyanin hexA and hexB in the asymmetric unit. The unique packing brings the PCB β155 very close together. The length unit is Å. The figure was created using the program *MOLSCRIPT* (Kraulis, 1991) and rendered with *Raster3D* (Merritt & Murphy, 1994).

energy transfer in C-phycocyanin discussed above is also connected with the β155 chromophore. The β155 chromophores in phycobilisome rods have dual function. In the phycobiliprotein hexamers, they absorb energy and transfer it to the β84 chromophore. The β155 chromophore also plays an important role for the lateral energy transfer between adjacent phycobiliprotein hexamers.

References

Apt, K. E., Collier, J. L. & Grossman, A. R. (1995). *J. Mol. Biol.* **248**, 79–96.

Brejc, K., Ficner, R., Huber, R. & Stenbacher, S. (1995). *J. Mol. Biol.* **249**, 424–440.

Brünger, A. T. (1992). *X-PLOR Version* 3.0: *A System for Crystallography and NMR.* Yale University, New Haven, CT, USA.

Brünger, A. T. (1997). *Methods Enzymol.* **277**, 243–269.

Bryant, D. A. (1991). *The Photosynthetic Apparatus, Molecular Biology and Operation, Cell Culture and Somatic Cell Genetics of Plants*, Vol. 7B, edited by L. Bogorad & I. K. Vasil, pp. 255–298. New York: Academic Press.

Chang, W., Jiang, T., Wan, Z., Zhang, J., Yang, Z. & Liang, D. (1996). *J. Mol. Biol.* **262**, 721–731.

Collaborative Computional Project, Number 4 (1994). *Acta Cryst.* D**50**, 760–763.

Debreczeny, M. P., Sauer, K., Zhou, J. & Bryant, D. A. (1993). *J. Phys. Chem.* **97**, 9852–9862.

Debreczeny, M. P., Sauer, K., Zhou, J. & Bryant, D. A. (1995*a*). *J. Phys. Chem.* **99**, 8412–8419.

Debreczeny, M. P., Sauer, K., Zhou, J. & Bryant, D. A. (1995*b*). *J. Phys. Chem.* **99**, 8420–8431.

Duerring, M., Schmidt, G. B. & Huber, R. (1991). *J. Mol. Biol.* **217**, 557–591.

Engh, R. A. & Huber, R. (1991). *Acta Cryst.* A**47**, 392–400.

Ficner, R., Lobeck, K., Schmidt, G. & Huber, R. (1992). *J. Mol. Biol.* **228**, 935–950.

Förster, T. (1967). *Comprehensive Biochemistry*, Vol. 22, edited by M. Florkin & E. H. Stotz, pp. 61–80. Amsterdam: Elsevier.

Gantt, E. (1990). *Biology of Red Algae*, edited by K. M. Coles & R. G. Sheath, pp. 203–219. Cambridge University Press.

Glazer, A. N. (1985). *Annu. Rev. Biophys. Chem.* **14**, 44–77.

Glazer, A. N. (1989). *J. Biol. Chem.* **264**, 1–4.

Glazer, A. N. & Melis, A. (1987). *Annu. Rev. Plant Physiol.* **38**, 11–45.

Jiang, J. S. & Brünger, A. T. (1994). *J. Mol. Biol.* **243**, 100–115.

Jiang, T., Zhang, J. P. & Liang, D. C. (1999). *Proteins Struct. Funct. Genet.* **34**, 334–231.

Jones, T. A., Zou, J. Y., Cowan, S. W. & Kjeldgaard, M. (1991). *Acta Cryst.* A**47**, 110–119.

Kraulis, P. J. (1991). *J. Appl. Cryst.* **24**, 946–950.

Laskowski, R. A., MacArthur, M. W., Moss, D. S. & Thornton, J. M. (1993). *J. Appl. Cryst.* **26**, 283–291.

Liu, J., Jiang, T., Zhang, J. & Liang, D. (1999). *J. Biol. Chem.* **274**, 16945–16952.

MacColl, R. (1998). *J. Struct. Biol.* **124**, 311–334.

MacColl, R. & Guard-Friar, D. (1987). *Phycobiliproteins.* Boca Raton, FL, USA: CRC Press.

Matthews, B. W. (1968). *J. Mol. Biol.* **33**, 491–497.

Merritt, E. A. & Murphy, M. E. P. (1994). *Acta Cryst.* D**50**, 869–873.

Navaza, J. (1994). *Acta Cryst.* A**50**, 157–163.

Otwinowski, Z. & Minor, W. (1997). *Methods Enzymol.* **276**, 307–326.

Ramachandran, G. N., Ramakrishnan, C. & Sasisekharan, V. (1963). *J. Mol. Biol.* **7**, 95–99.

Reuter, W., Wiegand, G., Huber, R. & Than, M. E. (1999). *Proc. Natl Acad. Sci. USA*, **96**, 1363–1368.

Ritter, S., Hiller, R. G., Wrench, P. M., Welte, W. & Diederichs, K. (1999). *J. Struct. Biol.* **126**, 86–97.

Sakabe, N. (1991). *Instrum. Methods Phys. Res. A*, **303**, 448–463.

Scheer, H. & Kufer, W. (1977). *Z. Naturforsch. C*, **32**, 513–519.

Schirmer, T., Bode, W., Huber, R., Silder, W. & Zuber, H. (1985). *J. Mol. Biol.* **184**, 257–277.

Schirmer, T., Huber, R., Schneider, M., Bode, W., Miller, M. & Hacket, M. L. (1986). *J. Mol. Biol.* **188**, 651–676.

Stec, B., Troxler, R. F. & Teeter, M. M. (1999). *Biophys. J.* **76**, 2912–2921.

Swanson, R. V. & Glazer, A. N. (1990). *J. Mol. Biol.* **214**, 787–796.

Zhang, J. P., Wan, Z. L., Wang, S. G., Chang, W. R. & Liang, D. C. (1995). *Acta Biophys. Sin.* **4**, 481–484.